Systematic ^{63}Cu NQR and ^{89}Y NMR Study of Spin Dynamics in $Y_{1-z}Ca_zBa_2Cu_3O_y$ across the Superconductor-Insulator Boundary

P. M. Singer and T. Imai

Department of Physics and Center for Materials Science and Engineering, MIT, Cambridge, Massachusetts 02139

(Received 12 December 2001; published 19 April 2002)

We demonstrate that the spin dynamics in underdoped $Y_{1-z}Ca_zBa_2Cu_3O_y$ for $y \simeq 6.0$ exhibit qualitatively the same behavior to underdoped $La_{2-x}Sr_xCuO_4$ for an equal amount of hole concentration $p = z/2 = x \le 0.11$. However, a *spin gap* appears as more holes are doped into the CuO_2 plane by increasing the oxygen concentration to $y \simeq 6.5$ for a fixed value of Ca concentration z. Our results also suggest that Ca doping causes disorder effects that enhance the low frequency spin fluctuations.

DOI: 10.1103/PhysRevLett.88.187601 PACS numbers: 76.60.–k, 74.25.Dw, 74.72.Bk

The mechanism of high temperature superconductivity remains a major mystery in condensed matter physics. The fundamental difficulty stems from the complexity of the electronic phase diagram, particularly in the underdoped region. Earlier ^{63}Cu NMR (nuclear magnetic resonance) and NQR (nuclear quadrupole resonance) measurements of the nuclear spin-lattice relaxation rate $^{63}1/T_1$ led to the discovery of the *pseudogap* phenomenon in the spin excitation spectrum of bilayer (Y, La)$Ba_2Cu_3O_y$ [1–4]. In the *spin pseudogap,* or *spin-gap* regime, low energy spin excitations are suppressed below the spin-gap temperature T^* ($>T_c$) which results in a decrease in $^{63}1/T_1T$ ($^{63}1/T_1$ divided by temperature T) below T^*. Subsequent NMR and optical charge transport measurements showed that a pseudogap appears both in the spin and charge excitation spectra of a wide variety of high T_c cuprates [5–9], with the most notable exception being the prototype high T_c cuprate $La_{2-x}Sr_xCuO_4$. Moreover, the temperature scale T^* of the spin gap and the charge gap increases with decreasing hole concentration towards the superconductor-insulator boundary [3,6,7,9].

In various theoretical model analysis, the pseudogap is often considered the key in understanding the mechanism of superconductivity. Unfortunately, driving CuO_2 planes into the insulating regime in a controlled fashion is technically difficult in many high T_c cuprates. As such, the fate of the pseudogap in the heavily underdoped insulating regime has been highly controversial. Attempts have been made to infer information on the spin gap based on uniform spin susceptibility $\chi'(\mathbf{q} = \mathbf{0})$ [10,11]. However, it is important to realize that growth of short range spin order alone causes a reduction of $\chi'(\mathbf{q} = \mathbf{0})$ *without* having any gaps. For example, the undoped CuO_2 plane shows a roughly linear decrease of $\chi'(\mathbf{q} = \mathbf{0})$ with decreasing temperature which is entirely consistent with the 2D Heisenberg model. By continuity, it is natural to associate the decrease of $\chi'(\mathbf{q} = \mathbf{0})$ in the heavily underdoped regime to be mostly due to growth of short range order with an effective energy scale $J(p)$ [12], and not to a spin gap.

It has also become increasingly popular to infer T^* for the charge sector based on scaling analysis of the Hall effect [10] or resistivity data [13]. Some authors claim that there is a universal phase diagram of T^* with p and T being the only two parameters, even in $La_{2-x}Sr_xCuO_4$. However, earlier ^{63}Cu NQR [14,15] and neutron scattering [16] experiments revealed no hint of a spin gap above T_c in $La_{2-x}Sr_xCuO_4$. Instead, $La_{2-x}Sr_xCuO_4$ exhibits an instability at low temperatures towards the formation of the quasistatic *stripe* with incommensurate spin and charge density waves [17–19]. Careful NMR (NQR) experiments of spin-gap effects with controlled doping near the superconductor-insulator boundary are necessary and would allow for comparison with $La_{2-x}Sr_xCuO_4$.

In this Letter, we report a systematic microscopic investigation of $Y_{1-z}Ca_zBa_2Cu_3O_y$ utilizing ^{63}Cu NQR and ^{89}Y NMR. The advantage of the $Y_{1-z}Ca_zBa_2Cu_3O_y$ system is that one can control the hole concentration near the superconductor-insulator boundary by fixing $y \simeq 6.0$ and varying z. In this case, the hole concentration is given by $p = z/2$, because the chain Cu sites [Cu(1)] with twofold oxygen coordination remain insulating with a 3d^{10} configuration [20]. In Fig. 1(a) we show the *absence* of a spin-gap signature in heavily underdoped $Y_{1-z}Ca_zBa_2Cu_3O_{6.0}$ ($z \le 0.22$) based on measurements of $^{63}1/T_1T$ at the

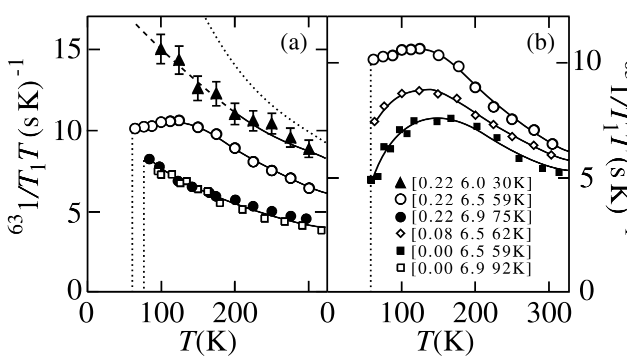

FIG. 1. (a) $^{63}1/T_1T$ above T_c (vertical lines) at the ^{63}Cu(2) site for $Y_{1-z}Ca_zBa_2Cu_3O_y$ [where [z y T_c] for each symbol is indicated in (b)], and for $La_{1.885}Sr_{0.115}CuO_4$ (dotted curve). (■) and (□) are taken from [21]. All lines are a guide for the eye. The dashed line through (▲) indicates region below $T_{\rm wipeout}$ where only partial Cu(2) signal intensity is observable.

planar Cu site [Cu(2)]. Instead, we show that the low energy spin excitations exhibit similar behavior to underdoped $La_{2-x}Sr_xCuO_4$, with equivalent $p = z/2 = x$, which monotonically grow with decreasing p and T. With further hole doping $Y_{1-z}Ca_zBa_2Cu_3O_{6.0}$ by oxygen loading to $y \simeq 6.5$ for fixed z, however, we *do* observe the spin-gap signature [Fig. 1(a)], even though it appears somewhat suppressed compared to $YBa_2Cu_3O_{6.5}$ without Ca substitution [Fig. 1(b)]. This is the first time in the high T_c cuprates where the appearance of a spin-gap signature is experimentally tracked through the insulator-superconductor boundary by increasing the hole doping. We recall that in contrast with the present case, further hole doping $La_{2-x}Sr_xCuO_4$ (or $La_2CuO_{4+\delta}$) does *not* result in a spin-gap signature; therefore our finding challenges the popular argument that charge disorder caused by the alloying effects of Sr^{+2} substitution (i.e., "dirt effects") *alone* suppresses the spin gap and drives $La_{2-x}Sr_xCuO_4$ towards the stripe instability.

We synthesized our polycrystalline samples following [22]. The oxygen concentration was controlled and determined following [23] with precision $\Delta y \sim \pm 0.05$. The ^{63}Cu NQR spectrum of all our $Y_{1-z}Ca_zBa_2Cu_3O_y$ samples are very similar to earlier reports [20], and the superconducting transition temperature T_c, as determined by SQUID measurements, shows close agreement with [22]. The temperature dependence of $^{63}1/T_1$ was measured with NQR near the peak frequency of the ^{63}Cu(2) site at $\omega_n/2\pi \simeq 25.5$ MHz [20] by applying an inversion pulse prior to the spin echo sequence. A typical $\pi/2$-pulse width of 3 μs was used. NMR measurements at 9 T in uniaxially aligned powder gave identical results to NQR within uncertainties. $^{63}1/T_1T$ is given by

$$^{63}\frac{1}{T_1T} = \frac{2k_B}{g^2\mu_B^2\hbar^2}\sum_{\mathbf{q}} |^{63}A(\mathbf{q})|^2 \frac{\chi''(\mathbf{q},\omega_n)}{\omega_n}, \quad (1)$$

where $^{63}A(\mathbf{q})$ is the wave-vector dependent, geometrical form factor of the electron-nucleus hyperfine coupling [24,25]. As shown in Fig. 1(a), $^{63}1/T_1T$ in underdoped $Y_{1-z}Ca_zBa_2Cu_3O_{6.0}$ ($z \leq 0.22$) with nominal hole concentration $p \leq 0.11$ does *not* exhibit a spin gap. Instead, $^{63}1/T_1T$ grows with decreasing temperature, exhibiting similar values as $La_{2-x}Sr_xCuO_4$, shown in Fig. 2(a). The fact that $^{63}1/T_1T$ grows with decreasing temperature indicates that low energy spin excitations continue to increase with decreasing temperature. Moreover, the enhancement of low energy spin excitations below 300 K is followed by the decrease of the ^{63}Cu NQR signal intensity below $T_{\rm wipeout}$ ($\gtrsim$200 K), i.e., *wipeout* effects [29–31]. Wipeout effects can be caused by various mechanisms [29] including the presence of nearly localized free spins induced by hole localization (in analogy with Cu NMR wipeout in Cu metal imbedded with dilute Fe or Mn spins), as well as the onset of the glassy slowing down of stripes.

The temperature dependence of $\chi'(\mathbf{q}=\mathbf{0})$ was deduced from the spin contribution $^{89}K_{\rm spin} = D\chi'(\mathbf{q}=\mathbf{0})$ to the ^{89}Y NMR Knight shift,

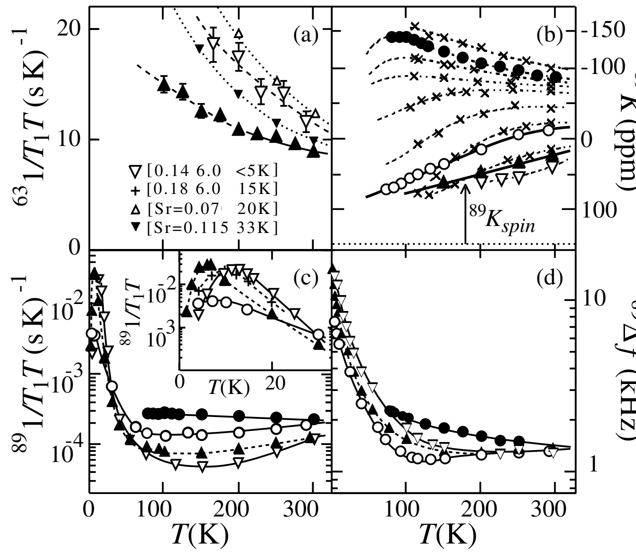

FIG. 2. The same symbol assignment as Fig. 1 is used, and new symbols are shown. (a) $^{63}1/T_1T$ in $Y_{1-z}Ca_zBa_2Cu_3O_y$ and $La_{2-x}Sr_xCuO_4$. (b) $\chi'(\mathbf{q}=\mathbf{0})$ in $Y_{1-z}Ca_zBa_2Cu_3O_y$ as measured by the ^{89}Y NMR Knight shift (^{89}K) taken above $T_{89}^{\rm min}$ [26] with respect to a YCl_3 reference. Data ($\times$) from [27] are a series of [0.20 y T_c] samples with T_c = 47.5, 65.8, 83.2, 86, 72.1, 60, and 47.5 K (in order of increasing $|^{89}K_{\rm spin}|$). The arrow indicates net spin contribution $^{89}K_{\rm spin}$. Solid lines are fits to the 2D Heisenberg model [28], and all other lines in the figure are guides for the eye. (c) $^{89}1/T_1T$ (with the same data plotted below 30 K in the inset) and (d) full width at half maximum $^{89}\Delta f$ of the ^{89}Y NMR line shape.

$$^{89}K = {}^{89}K_{\rm orb} + {}^{89}K_{\rm spin} \quad (2)$$

as shown in Fig. 2(b), where the powder averaged orbital contribution is $^{89}K_{\rm orb} = +150 \pm 5$ ppm [32] and D (<0) is the hyperfine coupling constant. Our ^{89}K data, taken in a magnetic field of 9 T, for $Y_{0.78}Ca_{0.22}Ba_2Cu_3O_y$ are consistent with earlier results reported above $\sim$110 K for $Y_{0.8}Ca_{0.2}Ba_2Cu_3O_y$ [27] also shown in Fig. 2(b). Our new measurement conducted down to $T_c = 75$ K in $Y_{0.78}Ca_{0.22}Ba_2Cu_3O_{6.9}$ shows a clear signature of saturation *below* 100 K, similar to overdoped $YBa_2Cu_3O_7$ without Ca substitution [33]. The saturation of $\chi'(\mathbf{q}=\mathbf{0})$ below 100 K is followed by a broad maximum at $T_{\rm max} = 90 \pm 10$ K, which according to the 2D Heisenberg model [28], implies an effective energy scale $J(p) = T_{\rm max}/0.93 = 97 \pm 11$ K. We also deduce $J(p)$ in underdoped $Y_{0.78}Ca_{0.22}Ba_2Cu_3O_{6.0}$ and $Y_{0.78}Ca_{0.22}Ba_2Cu_3O_{6.5}$ by matching $\chi'(\mathbf{q}=\mathbf{0})$ to the low temperature [$T \ll J(p)$] portion of the 2D Heisenberg model, as shown in Fig. 2(b). Our results of $J(p)$ (Fig. 3) are consistent with those reported in $La_{2-x}Sr_xCuO_4$ [12].

The ^{89}Y NMR data also show evidence for the glassy slowing of disordered magnetism. Below the onset of glassy slowing at $T_{\rm wipeout}$ ($\gtrsim$200 K), we find a change in curvature of $^{89}1/T_1T$ and an increase in $^{89}\Delta f$, as shown in Figs. 2(c) and 2(d), respectively [35]. The change in

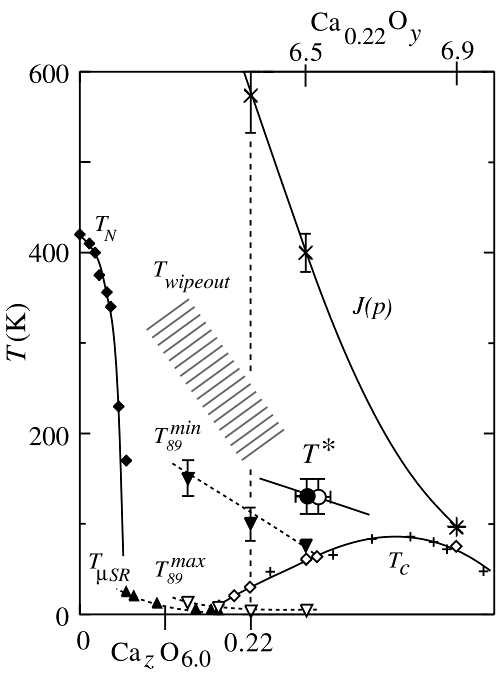

FIG. 3. Phase diagram of $Y_{1-z}Ca_zBa_2Cu_3O_y$ as a function of Ca_z substitution for fixed $y \simeq 6.0$ to the left of the dashed vertical line, and as a function of O_y concentration for fixed $z = 0.22$ to the right. The data includes T_N (◆) [22], $T_{\mu SR}$ (▲) [34], $T_{89}^{\min}$ (▼), $T_{89}^{\max}$ (▽), T_{wipeout} (hatched region), T^* (●), T_c (◇), and $J(p)$ (*, ×) deduced according to $T_{\max}$ and fit to the 2D Heisenberg model, respectively. Data to the right, including T_c (+) from [27], are positioned according to $|^{89}K_{\mathrm{spin}}|$ at 300 K. All lines are a guide for the eye and (○) is T^* for [0.08 6.5 62 K].

curvature of $^{89}1/T_1T$ is first followed by a minimum at $T_{89}^{\min}$ [26], and then a maximum at $T_{89}^{\max}$ where the glassy slowing has reached the NMR time scale. At a similar temperature $T_{\mu SR}$, μSR measurements observe local hyperfine fields [34] that are frozen on the μSR time scale. The enhanced values of $^{89}\Delta f$ at 1.7 K also indicate that the frozen hyperfine fields at the ^{89}Y nuclear site have a substantial spatial distribution of $\sim$70 Oe.

The sequence of anomalies starting at T_{wipeout} followed by $T_{89}^{\min}$, $T_{89}^{\max}$, and $T_{\mu SR}$ (Fig. 3) are analogous to $La_{2-x}Sr_xCuO_4$ where the onset of glassy slowing down of the stripe phase at T_{wipeout} [29–31] is followed by a minimum, then a maximum in $^{139}1/T_1T$ [36] and μSR observation of frozen hyperfine fields [34]. These sets of results establish the following three points: First, the paramagnetic Cu spin fluctuations in underdoped CuO_2 planes exhibit nearly universal p and T dependences in $Y_{1-z}Ca_zBa_2Cu_3O_{6.0}$ and $La_{2-x}Sr_xCuO_4$ for equivalent $p = z/2 = x$, *without* a pseudogap signature. In the same temperature range, the ^{89}Y NMR Knight shift decreases monotonically and is most likely due to the growth of short range spin order. Second, the gradual slowing of Cu spin fluctuations, as observed by the increase in $^{63}1/T_1T$, is followed by glassy freezing of the Cu moments starting at $T_{\mathrm{wipeout}} \sim 200$ K in $Y_{1-z}Ca_zBa_2Cu_3O_{6.0}$ while similar behavior is observed only below $\sim$100 K in $La_{2-x}Sr_xCuO_4$. The factor of 2 higher temperature scale is consistent with the finding based on μSR that the spin freezing temperature $T_{\mu SR}$ in $Y_{1-z}Ca_zBa_2Cu_3O_{6.0}$ is also a factor $\sim$2 higher than in $La_{2-x}Sr_xCuO_4$ [34]. Recalling that the Néel temperature of $T_N = 420$ K in undoped $YBa_2Cu_3O_{6.0}$ is higher than $T_N = 320$ K in La_2CuO_4 because of the bilayer coupling, the higher temperature scale of glassy spin freezing in $Y_{1-z}Ca_zBa_2Cu_3O_{6.0}$ may also be due to the stronger 3D coupling along the c axis. However, we cannot rule out the possibility that Ca^{+2} substitution causes stronger disorder in $Y_{1-z}Ca_zBa_2Cu_3O_{6.0}$ than Sr^{+2} substitution in $La_{2-x}Sr_xCuO_4$, as suggested by the factor $\sim$2 broader ^{63}Cu NQR spectrum [20], which may enhance the tendency towards spin freezing. Third, the observed increase of $^{89}1/T_1T$ implies that the Cu moments are not slowing down towards the commensurate antiferromagnetic spin structure with divergently large spin-spin correlation length. In this context, it is important to recall that the critical slowing down towards the Néel state does not cause a large enhancement of $^{89}1/T_1T$ in undoped $YBa_2Cu_3O_{6.0}$ [37] since the hyperfine form factor $^{89}A(\mathbf{q})$ is zero for the commensurate wave vectors. The strong increase of $^{89}1/T_1T$ shows that either the spin structure is incommensurate, as expected for the stripe phase, or that the spin-spin correlation length is limited to a relatively short length scale due to disorder caused by the holes, or possibly both. Since stripes are dynamic at NMR time scales even at $\sim$350 mK as evidenced by motional narrowing effects [31], our NMR data cannot distinguish the spin configuration.

We have established that the slowing of the paramagnetic spin dynamics in $Y_{1-z}Ca_zBa_2Cu_3O_{6.0}$ is qualitatively similar to $La_{2-x}Sr_xCuO_4$. Most importantly, we do not observe the signature of a spin gap. Instead, we find signatures of glassy slowing of spin fluctuations similar to the case of $La_{2-x}Sr_xCuO_4$. We caution that the absence of a spin-gap signature in the form of a decrease in $^{63}1/T_1T$ does not necessarily *prove* that there is no global suppression of lower energy parts of the spin fluctuations. $^{63}1/T_1T$ may grow monotonically with decreasing temperature as long as very low frequency ($\sim\omega_n$) components of the spin fluctuations grow, even if the global spin fluctuation spectrum is gapped below a certain temperature T^*. On the other hand, our result of T_{wipeout} sets an upper bound on T^* in $Y_{1-z}Ca_zBa_2Cu_3O_{6.0}$ because if T^* is significantly larger than T_{wipeout}, we should observe the decrease of $^{63}1/T_1T$ prior to the influence of glassy slowing of the spin dynamics which become visible below T_{wipeout}. Our conclusion that the magnitude of T^* is at most comparable to T_{wipeout} in $Y_{1-z}Ca_zBa_2Cu_3O_{6.0}$ is at odds with popularly held speculations, often based on theoretical expectations or more indirect experimental information such as the Hall effect, resistivity, and $\chi'(\mathbf{q} = \mathbf{0})$, that T^* blows up towards $J(p = 0) \sim 1500$ K.

A potential common cause of the absence of the spin-gap signature in underdoped $Y_{1-z}Ca_zBa_2Cu_3O_{6.0}$ and

$La_{2-x}Sr_xCuO_4$ is the random charge potential and/or disorder induced by substitution of Ca^{+2} or Sr^{+2} ions into Y^{+3} or La^{+3} sites, respectively. It is worth recalling that the absence of a spin-gap signature in $La_{2-x}Sr_xCuO_4$ has often been attributed to dirt effects caused by Sr^{+2}. However, our results in Fig. 1(a) also indicate that disorder *alone* does not entirely suppress the spin gap. Because of the solubility limit of Ca^{2+} into $Y_{1-z}Ca_zBa_2Cu_3O_{6.0}$ with a maximum $T_c \simeq 30$ K [22], we doped more holes into $Y_{0.78}Ca_{0.22}Ba_2Cu_3O_{6.0}$ by adding oxygen into the chain layers for the *same* sample to obtain $Y_{0.78}Ca_{0.22}Ba_2Cu_3O_{6.50}$ with $T_c \simeq 59$ K. We found that $^{63}1/T_1T$ in $Y_{0.78}Ca_{0.22}Ba_2Cu_3O_{6.50}$ decreases below $T^* \sim 130$ K, similar to the spin-gap signature in $YBa_2Cu_3O_{6.50}$ [3,21]. The data therefore suggest that the spin gap *does* develop when more holes are added into the CuO_2 plane in $Y_{0.78}Ca_{0.22}Ba_2Cu_3O_y$, even if the disorder effects caused by Ca doping tend to suppress the spin-gap signature.

For a more systematic study of the effects of Ca substitution alone, we compare $^{63}1/T_1T$ for $z = 0$, 0.08, and 0.22, with fixed $y = 6.50$–6.55 [Fig. 1(b)]. $^{63}1/T_1T$ is systematically enhanced with increasing z, especially at lower temperatures. Our data suggest that Ca^{+2} doping not only introduces holes but also tends to fill in the low frequency parts of spin fluctuations spectrum, without affecting the magnitude of T^* significantly. The Ca^{2+} substitution effects for $y \simeq 6.5$ are in remarkable contrast with the lack of change in $^{63}1/T_1T$ observed for $y \simeq 6.9$, as presented in Fig. 1(a) [38]. It is interesting to note the qualitative similarity with the Zn substitution effects in $YBa_2Cu_3O_y$ [39]. ^{89}Y NMR data show that Zn substitution [39] causes ^{89}Y line splitting in $T_c \simeq 60$ K phase samples but causes only ^{89}Y NMR line broadening in the $T_c \simeq 90$ K phase. These results suggest that both random spinless impurities in the CuO_2 plane (Zn^{2+}) and random Coulomb potentials outside the CuO_2 plane (Ca^{2+}) are more effectively shielded by a larger number of holes in the overdoped region. We mention that a more detailed analysis of the ^{63}Cu(2) spin-lattice recovery, similar to that used for Zn doped $YBa_2Cu_4O_8$ [40], is unfortunately not possible in $Y_{1-z}Ca_zBa_2Cu_3O_y$ due to the small overlap (~1%) of the Cu(1) signal with very long $^{63}T_1$ [20].

To conclude, using both ^{63}Cu NQR and ^{89}Y NMR we demonstrate the remarkable similarity in the paramagnetic spin dynamics between $Y_{1-z}Ca_zBa_2Cu_3O_{6.0}$ and $La_{2-x}Sr_xCuO_4$ for an equivalent nominal hole concentration. We do not observe any signatures of a spin gap for $p = z/2 = x \leq 0.11$. Upon further hole doping by oxygen loading with fixed z, we demonstrate that a spin gap does develop. Combining all our data, we deduce a phase diagram which crosses the superconductor-insulator boundary and includes the spin-gap temperature T^*, the effective energy scale $J(p)$ ($\gg T^*$), and the glassy freezing of the spin dynamics. Our systematic study of Ca substitution effects also suggests that charge disorder caused by Ca^{+2} ions tends to suppress the spin-gap signature while keeping T^* ($<T_{\rm wipeout}$) roughly constant.

T. I. thanks M. Greven, C. Nayak, S. Chakravarty, and X.-G. Wen for inspiring this project. This work was supported by NSF DMR 99-71264 and NSF DMR 98-08941.

[1] M. Horvatić *et al.,* Phys. Rev. B **39**, 7332 (1989).
[2] W. W. Warren *et al.,* Phys. Rev. Lett. **62**, 1193 (1989).
[3] H. Yasuoka, T. Imai, and T. Shimizu, in *Strong Correlation and Superconductivity: Proceedings of the IBM Japan International Symposium, Mt. Fuji, Japan, 1989,* edited by H. Fukuyama, S. Maekawa, and A. P. Malozemoff (Springer-Verlag, Berlin, New York, 1989); also see A. Goto *et al.,* Phys. Rev. B **55**, 12 736 (1997); A. Goto *et al.,* J. Phys. Soc. Jpn. **65**, 3043 (1996).
[4] For pseudogap signature in ^{89}Y NMR data, see H. Alloul *et al.,* Phys. Rev. Lett. **63**, 1700 (1989).
[5] Z. Schlesinger *et al.,* Phys. Rev. Lett. **65**, 801 (1990).
[6] C. C. Homes *et al.,* Phys. Rev. Lett. **71**, 1645 (1993).
[7] Y. Itoh *et al.,* J. Phys. Soc. Jpn. **63**, 22 (1994); Y. Itoh *et al.,* J. Phys. Soc. Jpn. **65**, 3751 (1996).
[8] M.-H. Julien *et al.,* Phys. Rev. Lett. **76**, 4238 (1996).
[9] K. Ishida *et al.,* Phys. Rev. B **58**, R5960 (1998).
[10] H. Y. Hwang *et al.,* Phys. Rev. Lett. **72**, 2636 (1994).
[11] T. Nakano *et al.,* J. Phys. Soc. Jpn. **67**, 2622 (1998).
[12] D. C. Johnston, Phys. Rev. Lett. **62**, 957 (1989).
[13] J. R. Cooper *et al.,* Physica (Amsterdam) **341C**, 855 (2000).
[14] S. Ohsugi *et al.,* J. Phys. Soc. Jpn. **60**, 2351 (1991).
[15] T. Imai *et al.,* Phys. Rev. Lett. **70**, 1002 (1993).
[16] K. Yamada *et al.,* Phys. Rev. Lett. **75**, 1626 (1995).
[17] J. M. Tranquada *et al.,* Nature (London) **375**, 561 (1995).
[18] Y. S. Lee *et al.,* Phys. Rev. B **60**, 3643 (1999).
[19] S. Wakimoto *et al.,* Phys. Rev. B **63**, 172501 (2001).
[20] A. J. Vega *et al.,* Phys. Rev. B **39**, 2322 (1989); A. J. Vega *et al.,* Phys. Rev. B **40**, 8878 (1989).
[21] T. Imai *et al.,* Physica (Amsterdam) **162C**, 169 (1989).
[22] H. Casalta *et al.,* Physica (Amsterdam) **204C**, 331 (1993).
[23] Y. Ueda *et al.,* Physica (Amsterdam) **156C**, 281 (1988).
[24] T. Moriya, J. Phys. Soc. Jpn. **18**, 516 (1963).
[25] A. J. Millis *et al.,* Phys. Rev. B **42**, 167 (1990).
[26] $T_{89}^{\rm min}$ also signals the temperature below which $^{89}1/T_1T \propto {}^{89}K_{\rm spin}$ ($\propto {}^{89}\Delta f$) scaling [32] no longer holds.
[27] G. V. M. Williams *et al.,* Phys. Rev. B **54**, R6909 (1996); G. V. M. Williams *et al.,* Phys. Rev. B **57**, 8696 (1998).
[28] R. R. P. Singh *et al.,* Phys. Rev. B **42**, 996 (1990).
[29] A. W. Hunt *et al.,* Phys. Rev. Lett. **82**, 4300 (1999); also see T. Imai *et al.,* J. Phys. Soc. Jpn. **59**, 3846 (1989).
[30] P. M. Singer *et al.,* Phys. Rev. B **60**, 15 345 (1999).
[31] A. W. Hunt *et al.,* Phys. Rev. B **64**, 134525 (2001).
[32] H. Alloul *et al.,* Phys. Rev. Lett. **70**, 1171 (1993).
[33] T. Auler *et al.,* Phys. Rev. B **56**, 11 294 (1997).
[34] Ch. Niedermayer *et al.,* Phys. Rev. Lett. **80**, 3843 (1998).
[35] Independent ^{89}Y NMR data in $Y_{0.85}Ca_{0.15}Ba_2Cu_3O_{6.1}$ by A. Campana *et al.,* Int. J. Mod. Phys. B **14**, 2797 (2000) are consistent with our data.
[36] F. C. Chou *et al.,* Phys. Rev. Lett. **71**, 2323 (1993).
[37] T. Ohno *et al.,* J. Phys. Soc. Jpn. **60**, 2040 (1991).
[38] Cu data for $Y_{0.78}Ca_{0.22}Ba_2Cu_3O_{6.9}$ are consistent with G. V. M. Williams *et al.,* Phys. Rev. B **63**, 104514 (2001).
[39] A. V. Mahajan *et al.,* Eur. Phys. J. B **13**, 457 (2000).
[40] Y. Itoh *et al.,* J. Phys. Soc. Jpn. **70**, 1881 (2001).